Microwave plasma nitriding of pure iron

Enrique Camps[a)]
Instituto Nacional de Investigaciones Nucleares, Apdo. Postal 18-1027, 11801 México, D.F. México

Stephen Muhl, O. Alvarez-Fregoso, and J. A. Juarez-Islas
IIM-UNAM, Apdo. Postal 70-360, 04510 México, D.F. México

Oscar Olea
Facultad de Química, UAEM, Edo. Mex. México

Saúl Romero
ININ, depto. Acelerador, México, D.F. México

(Received 12 October 1998; accepted 14 December 1998)

This article presents the results of a study of the plasma characteristics of an electron cyclotron resonance plasma source used for nitriding pure Fe. Diagnostic measurements, using optical emission spectroscopy, Langmuir probes, and an ion analyzer, were recorded as functions of the working pressure ($2-8\times10^{-4}$ Torr) and the external magnetic field near the substrate (from the extremes of highly compressed and divergent plasma fluxes). It was observed that the plasma source is capable of producing high density discharges, about 5×10^{11} cm^{-3} and ion energies about 15–48 eV. The ion energy was highest for the case of a divergent plasma ($\sim$45 eV). The most abundant excited radicals produced in the N/H discharges were the NH, N_2 and N_2^+ species. Experiments for nitriding of Fe showed the formation of distinct material structures dependent on the plasma conditions. Conditions were found for which it was possible to form almost single phases of Fe_3N and $Fe_{16}N_2$ in the sample surface. © *1999 American Vacuum Society.*
[S0734-2101(99)02404-5]

I. INTRODUCTION

Interest in nitriding of metal surfaces has been rapidly growing as industry is continually demanding better functionality in the surface and near surface properties of metal components. Applications range from improvement of corrosion and wear resistance to modifications of electronic and magnetic properties. The use of high frequency plasmas has been seen to provide an enhancement of the more well-established conventional processes, including traditional gas and liquid nitriding. These improvements comprise mainly the reduction of treatment times and process control,[1,2] but an additional attractive feature of plasma nitriding is its greater environmental cleanliness.

Due to its remarkable mechanical and magnetic properties, the iron-nitrogen system has been studied for many decades. The initial interest in the Fe-N system came from the nitriding of steels to improve the abrasive strength by surface hardening.[3] In relation to the magnetic properties, of the iron nitrides $Fe_{16}N_2$ shows an extremely high saturation magnetization, 298 emu g^{-1},[3] a value which exceeds that of α-Fe. Ferromagnetic iron nitride compounds (Fe_xN, with $2\leqslant x \leqslant 8$) have a higher mechanical hardness, larger saturation magnetization, and superior chemical stability than those of pure iron. Many methods have been used to prepare iron nitride, such as iron metal nitriding,[4] sputtering,[5] ion plating,[6] molecular beam epitaxy,[7] ion beam deposition,[8] and ion implantation,[9] but there have been, as far as we are aware, no attempts to use a microwave discharge as we report here.

Low pressure plasmas with high densities of ions, radicals, and excited species can be easily formed using microwave electron cyclotron resonance (ECR) heating of a discharge. These types of plasma have been successfully used in thin film processes, such as deposition and etching by sputtering and plasma enhanced chemistry. In the field of plasma nitriding, there are few reports of the nitriding of steels (see for example Refs. 10 and 11). However, microwave discharges have important advantages for low pressure plasma processing, compared to conventional direct current (dc) or radio frequency (rf) discharges, including several orders of magnitude greater degree of ionization,[12] higher efficiency as they produce high densities without the need for high levels of energy,[13] and the generation of fast electrons, which results in higher electron temperatures.[14,15]

The advantages of microwave discharges are accompanied by some disadvantages, mainly related with the difficulties in establishing a good control of the plasma parameters. Basically by changing conditions such as, the working pressure, flow or type of gas, input power or the external magnetic field, changes occur in the plasma density, the electron temperature, the ion energy, and the amount and proportion of excited species. In the present article the characterization of a microwave ECR plasma source has been carried out in order to determine its characteristics as a function of some of the working parameters; magnetic field, gas pressure, and gas type. This is for regimes used to nitride pure iron. Finally we present the results of the treatment for different plasma conditions.

a)Electronic mail: camps@servidor.unam.mx

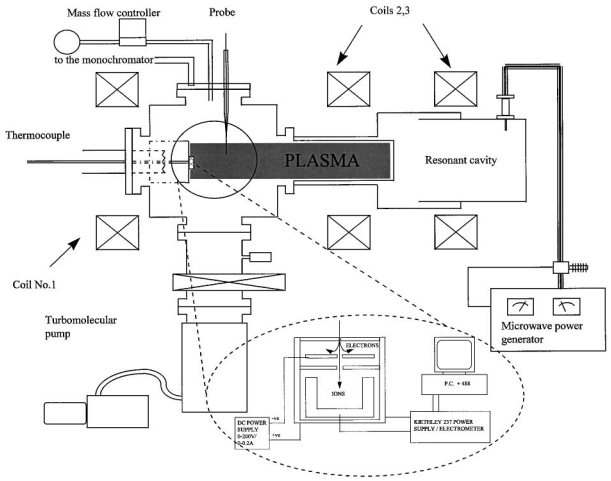

FIG. 1. Schematic drawing of the experimental equipment.

II. EXPERIMENTAL SETUP

The ECR microwave plasma source used in this work is shown schematically in Fig. 1, and was described in detail elsewhere.[15] Microwave radiation ($f=2.45$ GHz, 0–500 W) is introduced in continuous-wave mode into a variable length resonant cavity, inside of which is located a 6 cm diameter quartz tube containing the working gas. The typical base pressures was 5×10^{-6} Torr, and the processing pressures in the 10^{-4} Torr range. The system magnetic field is produced by three solenoid coils surrounding the discharge. The B field in the center of the resonant cavity is adjusted to a value of 875 G to ignite the plasma, and then reduced to almost half of the resonant value, in order to produce the highest value of plasma density. The field strength in the output of the device (i.e., near the substrate holder) can be varied independently, in order to create a compressed or a divergent plasma flux.

The electron plasma density (n_e), electron temperature (T_e), and potentials (V_p-plasma potential, V_f-floating potential) were measured using a cylindrical Langmuir probe with a 0.3 mm diam. tungsten tip, 5 mm long, located in the reaction chamber perpendicular to the plasma flux. In the region of the probe the magnetic field has a maximum value of ~200 G. Thus the condition $\rho_{ci}>\rho_{ce}>\rho_p$ (where $\rho_{ci,ce}$ is the Larmor radius of the ions and electrons and, ρ_p is the radius of the probe) is satisfied, and the ion saturation current collected at the probe can be considered to be undisturbed by the magnetic field, and the ion theory for the interpretation of the current–voltage ($I-V$) characteristic is applicable.[16]

The optical emission from the plasma was collected by an optical fiber bundle through a quartz window in the reaction chamber, and was analyzed using a 1/4m monochromator from Acton Research Corp., model Spectra Pro with a 2400 l/mm grating and a PD439 photomultiplier connected to a PC.

The ion energy was measured by means of an energy analyzer, consisting of two internal electrodes and an ion collection plate enclosed in a 2 cm diam stainless steel chamber. A 600 μm radius aperture in the top stainless steel membrane (~750 μm thick) of the analyzer was used to sample the ions impinging on the detector. The electrodes inside the analyzer had apertures of 1.0 and 1.5 mm diam for the upper and lower electrodes, respectively. The upper electrode was biased at −100 V dc to ensure that all electrons and negative ions in the plasma were repelled. The lower electrode is connected to ground. The potential applied to the ion collection electrode was varied from 0 to 120 V, thus permitting the energy analysis of the ions. All of the internal parts of the

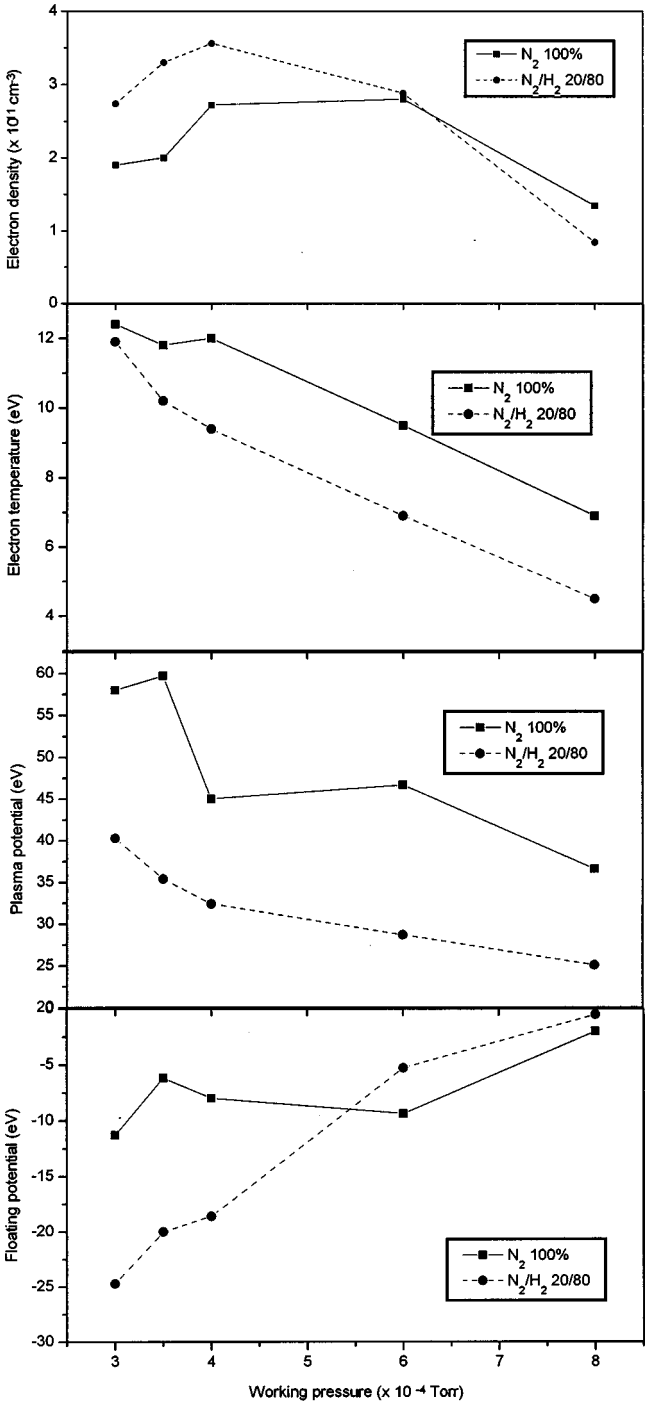

FIG. 2. Plasma parameters as a function of the working pressure, for different gas mixtures, in the compressed plasma regime.

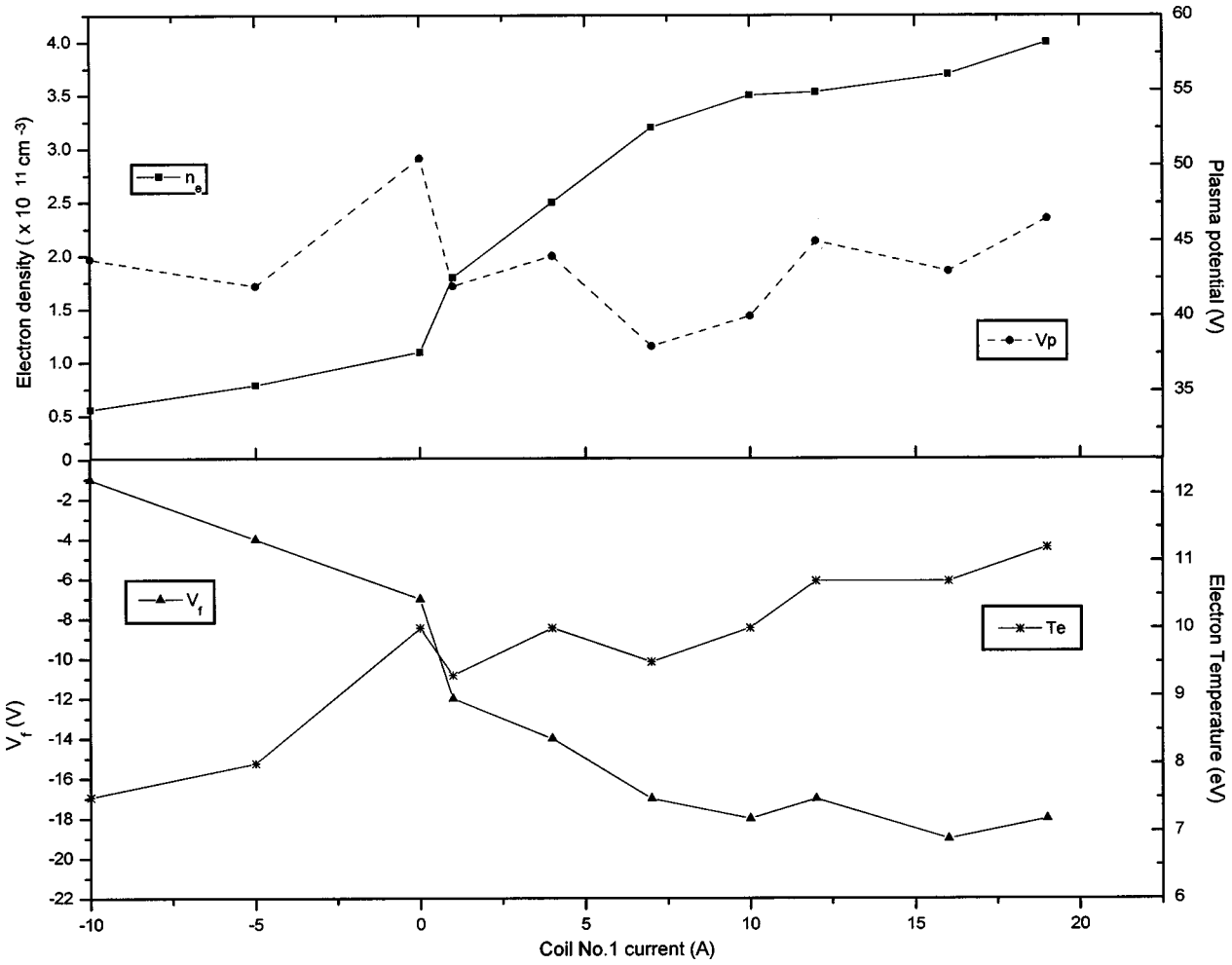

FIG. 3. Plasma parameters as a function of the magnetic field formed by coil 1, for the case of an argon discharge at 4×10^{-4} Torr.

analyzer are made of graphite to reduce the disturbance from secondary electron generated by ion impact. The ion current and retardation potential was measured and supplied using a Keithley 247 Source/Electrometer connected to and controlled by a PC. The energy distribution of the positive ions, $N(E)$, can be calculated from the collected ion current as a function of the ion retardation potential, by differentiating the total ion current with respect to the retardation potential.

A wide range of the system parameter space was characterized with the techniques described above and included those used to carry out the nitriding of pure Fe (99.9%). Prior to the treatment the samples were mirror polished, cleaned in methanol and characterized by microhardness measurements using a Matsuzawa MXT30-UL tester. The plasma used was of different mixtures of H_2 and N_2 with the gas flow controlled using MKS 247 mass flow controllers. Nitriding was carried out with the specimens in direct contact with the plasma and were electrically isolated from the chamber, thus during processing they are at the floating potential of the plasma. This procedure takes advantage of the naturally established difference between the plasma and floating potential to cause bombardment of the substrate. The temperature of the samples on their treated surface could be varied between 300 and 500 °C depending on the plasma conditions. The values of temperature used were calculated from calibration experiments involving the use of chromel-alumel thermocouples connected to both the front and back surfaces of a sample.

The morphology of the nitrided surface was examined using an atomic force microscope (Autoprobe, Park Sci. Instruments) in the contact mode. The microstructure of the cross section of the iron nitride/iron substrate interface was analyzed using a scanning electron microscope (SEM) (Leica-Cambridge 440). Crystalline and phase characterization was performed using a Siemens D-5000 x-ray diffractometer.

The relative surface concentration and maximum penetration of the nitrogen of some of the samples were measured by nuclear reaction analysis (NRA). A Tandem Van de Graaff accelerator was used to carry out the NRA measurements, using deuteron irradiation of the samples at 1800 and 2200 keV. The detection angle was 150° with the sample surface perpendicular to the ion beam. The nitrogen analysis was made using the $^{14}\mathrm{N}(d,p_o)^{15}\mathrm{N}$ and $^{14}\mathrm{N}(d,\alpha_o)^{12}\mathrm{C}$ nuclear reactions. Analysis of the experimental and simulated spectra

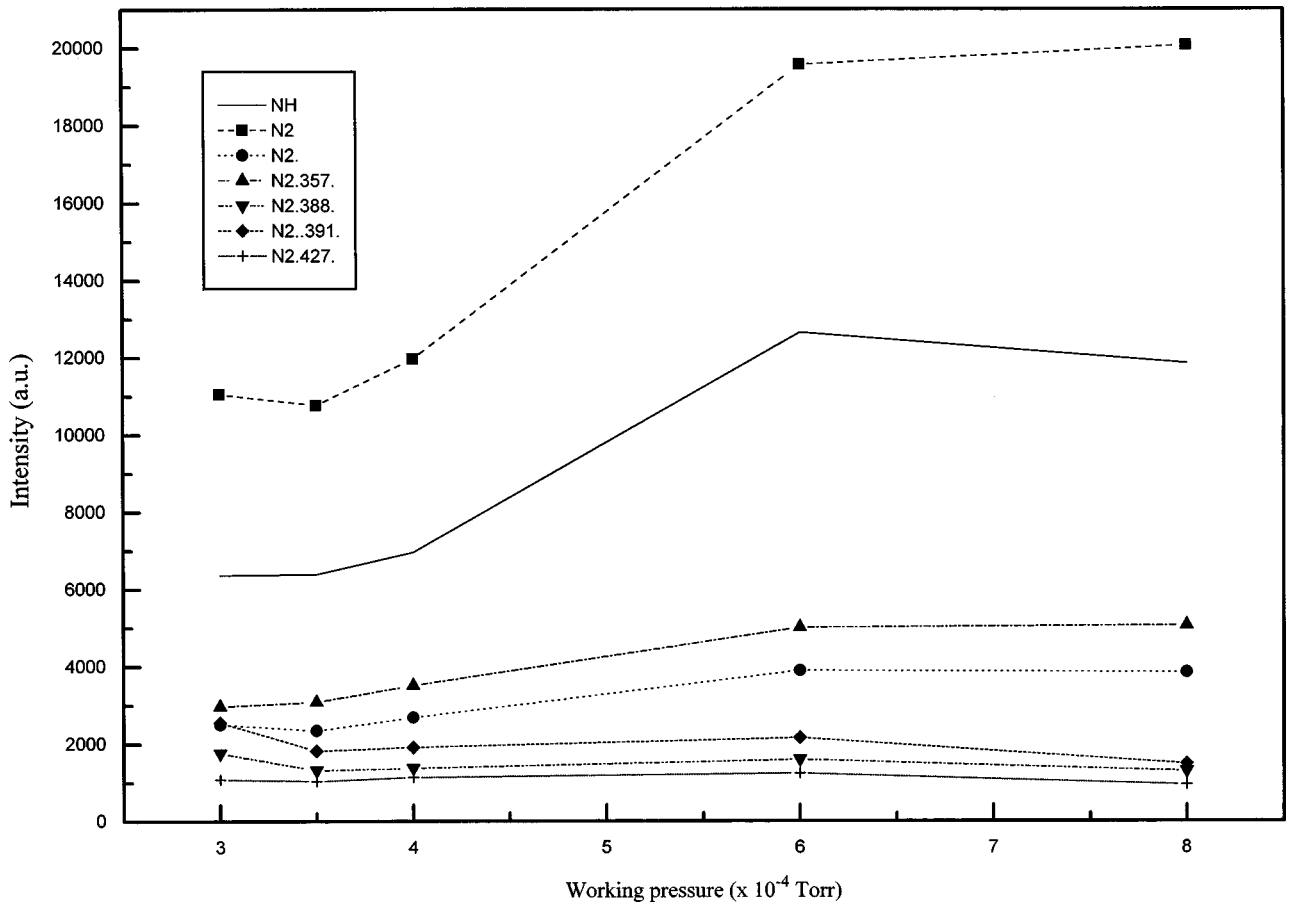

FIG. 4. Intensity of spectral lines, for the most intense peaks, as a function of the process pressure.

allowed the calculation of the nitrogen depth penetration profile.

III. RESULTS AND DISCUSSION

A. Plasma parameters

The plasma parameters were studied as functions of the process pressure and the magnetic field formed by the coil at the output of the device (i.e., coil 1), for different working gases (Ar, N_2, and mixtures N/H). For all the measurements given here the incident power was constant and fixed at 350 W, since almost no variations were detected, for greater values, up to the source maximum of 500 W. The value of the magnetic field in the resonant region (inside the resonator) strongly affects the plasma parameters, and therefore this was fixed at the value where the greatest density and the lower microwave reflection was achieved for each case (this was close to the half that of the resonant value).

Figure 2 shows typical plots of the plasma parameters for two different types of gases (N_2 100% and the mixture 20/80 N_2/H_2), versus gas pressure. From these graphs it can be seen that there exists a range, between 4 and 6×10^{-4} Torr, where the electron density is maximum, the exact pressure value depends on the type of gas used. The N_2 discharges showed somewhat lower values of density than those obtained with high amounts of hydrogen. On the other hand, electron temperatures are normally greater for the N_2 discharges. For all the gas types, T_e decreased when the pressure was increased, probably due to the increase of the number of collisions. The reduction of electron temperature also leads to a reduction of the plasma potential and to an increase of the floating potential (i.e., it becomes less negative). At the same time this reduces the electric field of the sheath, and because our samples are held at the plasma floating potential, they receive a less intense ion bombardment.

Figure 3 shows the plasma parameters as functions of the magnetic field created by coil 1. It should be noted that the negative values of current mean that a cusp magnetic field configuration is formed. At low positive values a divergent plasma flux is obtained and at high values ($\sim$20 A) the plasma is highly compressed. This figure shows that the overall behavior of the plasma is the same no matter what gas is used. It can be seen that the electron temperature and density decrease when the B field is reduced, the plasma potential is practically unaffected, the variation given that is within the experimental error, but the floating potential becomes less negative for the lower values of the field. The increase of electron temperature with higher magnetic fields is a consequence of a better magnetic confinement, this confinement means that the electrons can gain energy and that electron losses are reduced which increases the plasma density.

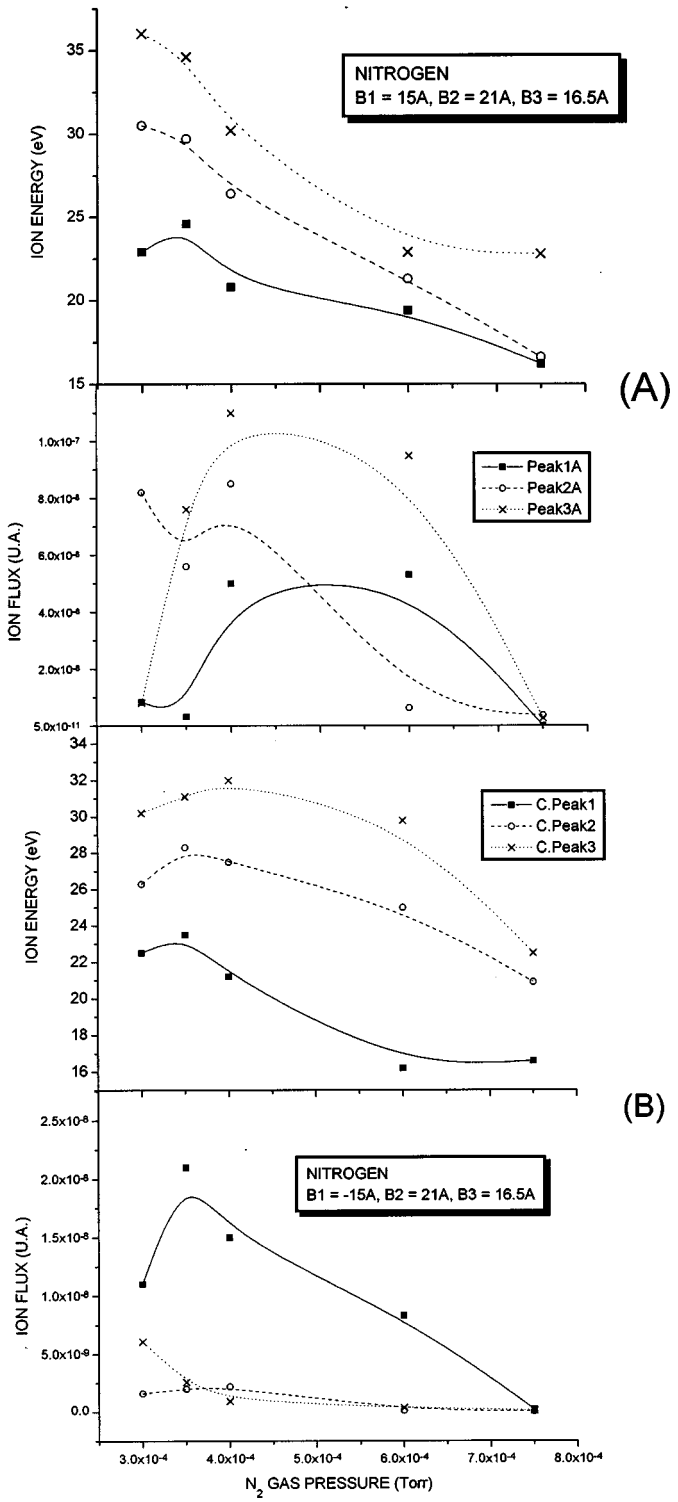

FIG. 5. Variation of ion energy and ion flux as a function of the nitrogen gas pressure. The parameter here is the coil 1 current.

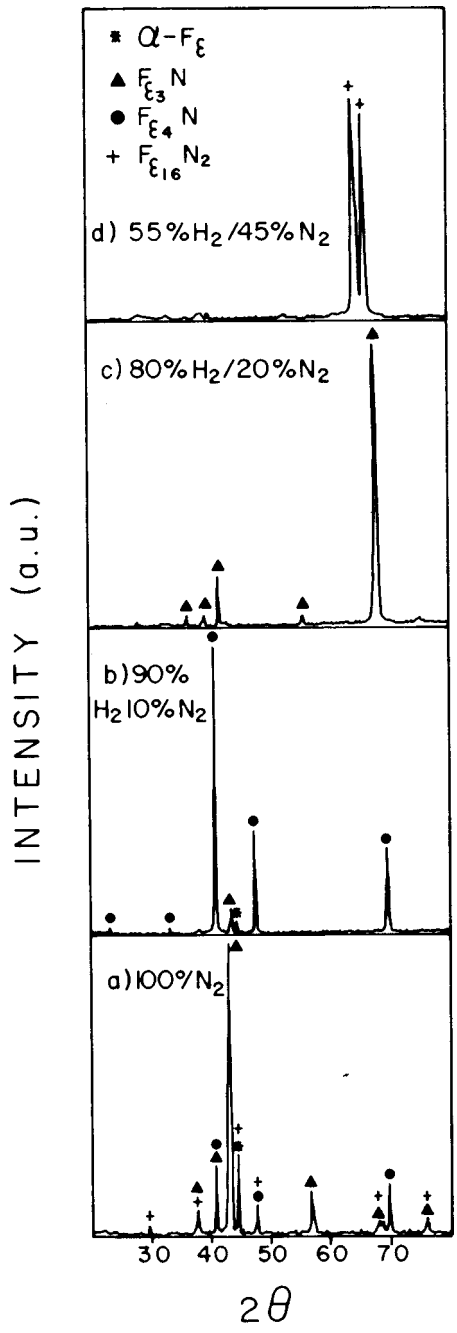

FIG. 6. Typical crystallographic XRD patterns for the FeN coatings grown with different plasma conditions.

Figures 2 and 3 are important to understand the ion energy changes as function of these parameters, which will be discussed in the section where the ion energy is measured.

B. Spectroscopic measurements

The optical emission spectra were obtained for the discharges with N_2 and its mixture with H_2, measured in the wavelength range from 300 to 450 nm. These measurements were performed simultaneously with the probe measurements, so that the incident power and magnetic field have the same values as for those measurements. In the spectra for N_2, were observed peaks in the near ultraviolet (UV) region centered at 316, 337, 380, and 400 nm, which correspond to the most intense peaks of the second positive system of the nitrogen molecule. The observed peaks 391 and 428 nm correspond to the first negative system of the N_2^+ transition. For the case of the described discharge, these latter are not the more intense ones, as seen in other types of plasma, such as for example the capacitive rf system described by Clay and

TABLE I. Crystallite shape, composition, and hardness of FeN coatings.

Sample morphology	Working gas	Coating composition ±3%	μHardness Hv (±10%)	
Cubes	100% N_2	$Fe_{2.29}N$	900	mixed phase
Rhombuses	10/90 N_2/H_2	$Fe_{4.01}N$	400	single phase
Needles	20/80 N_2/H_2	$Fe_{3.11}N$	340	single phase
Granules	55/45 N_2/H_2	$Fe_{15.84}N_2$	340	single phase

collaborators,[17] or the dc discharge described in Ref. 18. Although the peak exists, it is of lower intensity than the 337.1 peak, corresponding to the N_2 or the 336.1 of the NH, so we see that, the chemical species active in the ECR microwave discharge are different, and this basically due to the excitation method and the lower pressures used. Figure 4 shows the intensity of some of the lines observed in the recorded spectra plotted against working pressure. For 20/80 N_2/H_2 mixture, these graphics show the possibility of producing more excited species at higher values of pressure, where the plasma density tends to decrease. From these it appears that treatments at low sample temperatures are possible under conditions where the highest densities of neutral excited species are generated.

C. Ion energy measurements

Charged particles hitting the substrates may gain energy greater than their thermal energy, due to the plasma sheath potential established by the difference between the plasma potential and the potential attained by the samples (in the case of the nitriding this is the floating potential),[12] the spatial variations of the plasma potential and the gradients of the external magnetic field. The ion energies and flux were measured as a function of gas pressure and the magnetic field generated by coil 1, using pure argon or nitrogen. The peaks obtained in the dI/dV versus V graphs were normally found to be asymmetric Gaussians, with the asymmetry mainly on the low energy side. However, in some cases two or three distinct peaks were observed. The asymmetry has been observed by other groups and has been interpreted as arising from a lateral component in the velocity of the ions. We have found that a very good fit of the data can be obtained by supposing the existence of two or three different energy ion species, for argon and nitrogen, respectively. Although this procedure requires future work to establish that it is in fact correct, support is provided by the observation of resolved peaks under certain circumstances as well as from the optical emission results. Figures 5(a) and 5(b) show the variation of the ion energy and ion flux as a function of the nitrogen gas

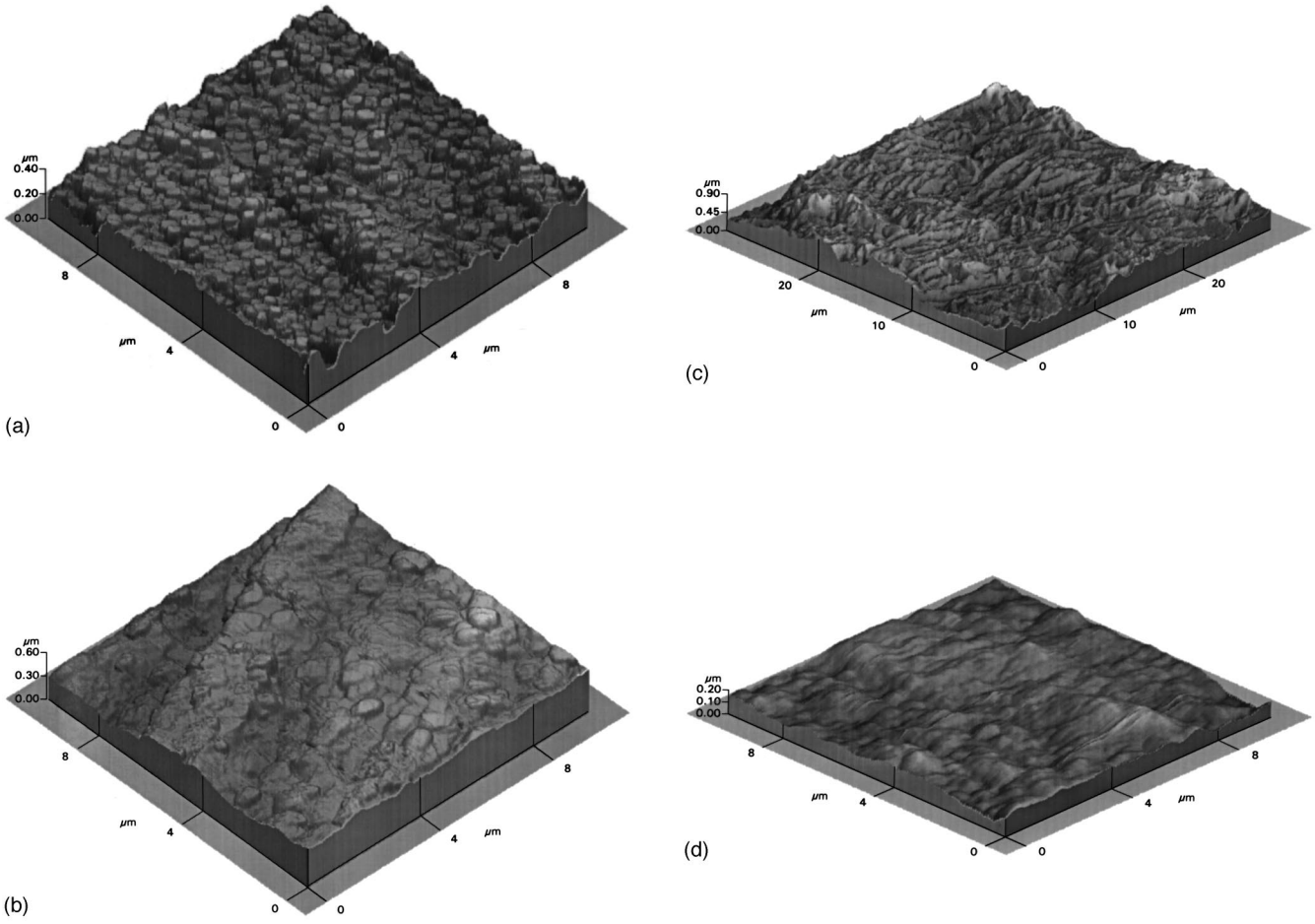

FIG. 7. Different crystallite shape of the samples analyzed in Fig. 6 (in the same order).

pressure for compressed and cusp plasma configurations, respectively. The results for argon were seen to be similar in form but the ion energies were 3–5 eV higher. The units of ion flux are not specified because the transmission efficiency of the ion analyzer is not known. For the compressed plasma the ion energy and one of the ion fluxes decrease strongly with increasing gas pressure. The flux of the other ions is high for pressures from 4 to 6×10^{-4} and much lower at higher and lower pressures. The situation can be seen to be very different for the cusp configuration; for two of the ion species there is little change in the ion energy up to 6×10^{-4} but the flux of these is quite small. The energy of the highest ion flux decreases strongly above 4×10^{-4} Torr, with a flux maximum at $3.5–4\times10^{-4}$ Torr. At present we have not been able to identify the three ion species, but using the emission data we can tentatively say, that the peaks 1, 2, and 3 correspond to ions of doubly ionized molecular nitrogen, NH (from the residual water vapor in the chamber) or atomic nitrogen, and singly ionized molecular nitrogen, respectively. At low magnetic fields created by coil 1 (divergent plasma regime), the ion energy decreases, as a consequence of the reduction in the difference of potentials between V_p and V_f, mainly by the reduction in V_f as it is shown in Fig. 3. The ion flux is also reduced in this case, because of the reduction of the plasma density (see Fig. 3). These results show that by varying the current in coil 1 the energy of ions can be changed, establishing a control on the energy of the particles that hit the substrates during the treatment of materials.

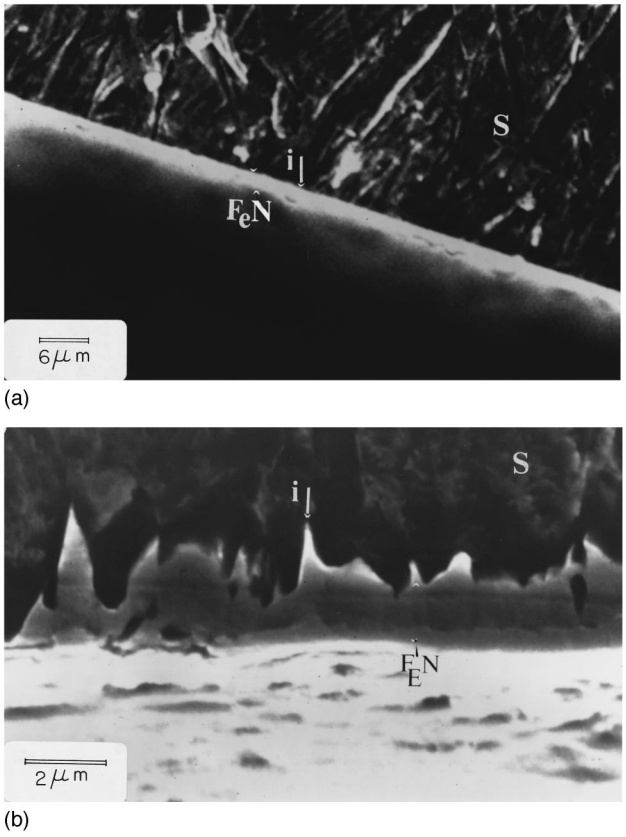

FIG. 8. Interface morphology imaged by SEM. (a) sharp-homogeneous, (b) diffusive-irregular interface.

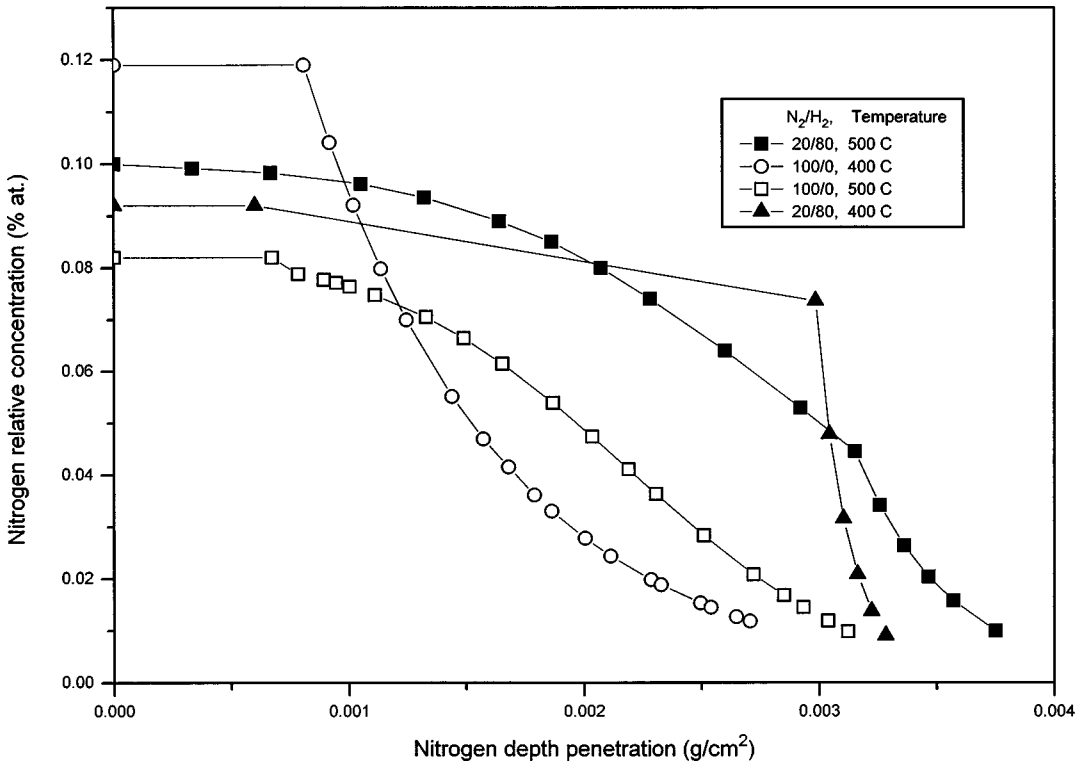

FIG. 9. Nitrogen relative concentration vs nitrogen depth penetration, obtained by NRA. Open symbols correspond to mixed phases, closed symbols to Fe_3N.

IV. NITRIDING OF PURE Fe

Typical crystallographic x-ray diffraction (XRD) patterns for FeN coatings grown in discharges with different working gases (different N/H mixtures) are shown in Fig. 6. In this figure are shown almost single phase Fe_3N, Fe_4N and $Fe_{16}N_2$ materials [Figs. 6(b)–6d)], and a mixed phase coating with random orientation [Fig. 6(a)], obtained using a discharge with 100% N_2 with an n_e of $\sim 2.5\times 10^{11}$ cm^{-3}, a T_e of ~ 12 eV, in the compressed plasma flux regime with a treatment time of 25 min, and an ion energy of ~ 35 eV. Under these conditions the sample achieved a temperature of 500 °C. Figure 6(b), shows the almost single phase Fe_4N with (1,1,1) orientation, obtained using the 10/90, N_2/H_2 mixture in the discharge, with an $n_e \sim 4.6\times 10^{11}$ cm^{-3}, and a T_e of 8 eV, in the compressed plasma regime, with an ion energy ~ 25 eV, a treatment time of 25 min, and a sample temperature of 500 °C. Figure 6(c) shows the XRD pattern for the almost single phase Fe_3N with (1,1,0) orientation, grown using the 20/80 N_2/H_2 mixture, with a plasma density of n_e of $\sim 3.5\times 10^{11}$ cm^{-3} and a $T_e \sim$ 9 eV, in the compressed regime with an ion energy of about 30 eV, 25 min treatment with a sample temperature of 500 °C. Figure 6(d) shows the pattern corresponding to the almost single phase $Fe_{16}N_2$ with (2,0,4)-(2,1,4) orientation, obtained using a 45/55 N_2/H_2 mixture, with an n_e of about 3×10^{11} cm^{-3}, a T_e of 9 eV, in the divergent plasma regime with an ion energy of 25 eV, carried out for 40 min with the sample at 370 °C.

These results show that using different mixtures of the working gas and appropriate experimental growth conditions, it is possible to produce FeN thin films with almost single phases. Table I gives a collection of some of the properties and experimental conditions for these experiments.

The surface morphology of FeN films was determined by atomic force microscopy and the depth penetration profiles of nitrogen by nuclear reaction analysis (NRA). Figure 7 illustrates the main changes in the crystallite shape for the same samples analyzed by XRD. The crystallites seen are cubic [Fig. 7(a)], rhombohedral [Fig. 7(b)], needle-like [Fig. 7(c)], or have a granular morphology [Fig. 7(d)]. We can conclude that the ECR microwave plasma systems appears to be a promising method to prepare a variety of surface coatings with very different surface topographies, grain sizes, and structures.

The film-substrate interface morphology was imaged by SEM. Figure 8 shows the diffusive irregular seen in the Fe_3N sample [Fig. 8(a)] and a sharp-homogeneous [Fig. 8(b)] interface observed in the mixed phases sample. The diffusive-irregular interface shape is possibly due to a skin layer of a molten iron region, similar to that reported by Ebisawa and Saikudo,[19] and its NRA profile is typical of a diffusive mechanism of the N, as is shown in Fig. 9 for some samples. The homogeneous sharp interface is characterized by a typical parabolic rate equation based on Fick's law for a fast volume diffusion process.

V. CONCLUSIONS

A microwave ECR discharge used in the nitration of materials has been characterized. Its main parameters, such as density, electron temperature, plasma, and floating potentials, were studied as functions of the pressure and magnetic field. Optical emission measurements showed that the main excited chemical species are different from those observed in other types of discharges (e.g., dc or rf). Measurements of the energies of the ion incident on the substrate indicated a dependence with the magnetic field at the output of the device. This aspect permits a certain degree of control of this parameter, without affecting the main discharge in the resonant cavity.

The plasma was used to nitride pure iron, and it was shown that the production of certain specific phases was possible. In particular, we have found that we could produce almost single phases of Fe_3N, Fe_4N, and $Fe_{16}N_2$. Knowledge of the details of the plasma parameters at which these materials were obtained is very important, not only because this can give information useable in the understanding of how the phases are formed, but also because this greatly enhanced the process reproducibility.

ACKNOWLEDGMENTS

This work was partially supported by CONACYT under Contract No. 3325P-A9607. The authors would like to thank Fidencio Estrada Gutiérrez for his technical support.

[1]B. Edenhofer, Heat Treat. Met. **1**, 23 (1974).
[2]E.I. Meletis and S. Yan, J. Vac. Sci. Technol. A **11**, 25 (1993).
[3]T. K. Kim and M. Takahashi, Appl. Phys. Lett. **20**, 492 (1972).
[4]R. N. Panda and N. S. Gajbhiye, J. Appl. Phys. **81**, 335 (1997).
[5]K. Oda, T. Yoshio, and K. Oda, J. Mater. Sci. **25**, 2557 (1990).
[6]K. Umeda, Y. Kawashimo, M. Nakasone, S. Harada, and A. Tasaki, Jpn. J. Appl. Phys., Part 1 **23**, 1576 (1984).
[7]M. Komuro, Y. Kozono, and Y. Sugita, J. Appl. Phys. **67**, 5126 (1990).
[8]N. Tarada, Y. Hoshi, M. Naoe, and S. Yamanaka, IEEE Trans. Magn. **20**, 1431 (1984).
[9]N. Nakajima, T. Yamashita, M. Takata, and S. Okamoto, J. Appl. Phys. **70**, 6033 (1991).
[10]M. K. Lei and Z. L. Zhang, J. Vac. Sci. Technol. A **13**, 2986 (1995).
[11]E. Camps, S. Muhl, S. Romero, and J.L. Garcia, Surf. Coat. Technol. **2/3**, 121 (1998).
[12]J. Hopwood, D. K. Reinhard, and J. Asmussen, J. Vac. Sci. Technol. A **8**, 3103 (1990).
[13]F. F. Chen, Phys. Plasmas **2**, 2164 (1995).
[14]J. Hopwood and J. Asmussen, Appl. Phys. Lett. **58**, 2473 (1991).
[15]E. Camps, O. Olea, C. Gutierrez-Tapia, and M. Villagran, Rev. Sci. Instrum. **66**, 3219 (1995).
[16]Yu. M. Kagan and V. I. Perel, Sov. Phys. Usp. **81**, 767 (1964).
[17]K. J. Clay, S. P. Speakeman, G. A. Amaratunga, and S. R. P. Silva, J. Appl. Phys. **79**, 7227 (1996).
[18]L. Petitjean and A. Ricard, J. Phys. D **17**, 919 (1984).
[19]T. Ebisawa and R. Saikudo, Surf. Coat. Technol. **86/87**, 622 (1996).